

Carbon Nanohorns as Effective Nanotherapeutics in Cancer Therapy

Author:

Curcio, Manuela; Cirillo, Giuseppe; Saletta, Federica; Michniewicz, Filip; Nicoletta, Fiore Pasquale; Vittorio, Orazio; Hampel, Silke; Iemma, Francesca

Publication details:

C-JOURNAL OF CARBON RESEARCH

v. 7

Chapter No. 1

2311-5629 (ISSN)

Publication Date:

2021-03-01

Publisher DOI:

<https://doi.org/10.3390/c7010003>

License:

<https://creativecommons.org/licenses/by-nc-nd/4.0/>

Link to license to see what you are allowed to do with this resource.

Downloaded from http://hdl.handle.net/1959.4/unsworks_80921 in <https://unsworks.unsw.edu.au> on 2024-05-18

Review

Carbon Nanohorns as Effective Nanotherapeutics in Cancer Therapy

Manuela Curcio ¹, Giuseppe Cirillo ^{1,*} , Federica Saletta ^{2,3}, Filip Michniewicz ^{2,3}, Fiore Pasquale Nicoletta ¹ ,
Orazio Vittorio ^{2,3,4,*}, Silke Hampel ⁵  and Francesca Iemma ¹

- ¹ Department of Pharmacy, Health and Nutritional Sciences, University of Calabria, 87036 Rende (CS), Italy; manuela.curcio@unical.it (M.C.); fiore.nicoletta@unical.it (F.P.N.); francesca.iemma@unical.it (F.I.)
- ² Children's Cancer Institute, Lowy Cancer Research Centre, UNSW Sydney, Randwick, NSW 2031, Australia; F.Saletta@ccia.org.au (F.S.); FMichniewicz@ccia.org.au (F.M.)
- ³ School of Women's and Children's Health, Faculty of Medicine, UNSW Sydney, NSW 2052, Australia
- ⁴ ARC Centre of Excellence for Convergent BioNano Science and Technology, Australian Centre for NanoMedicine, UNSW Sydney, NSW 2052, Australia
- ⁵ Leibniz Institute of Solid State and Material Research Dresden, 01069 Dresden, Germany; s.hampel@ifw-dresden.de
- * Correspondence: giuseppe.cirillo@unical.it (G.C.); OVittorio@ccia.unsw.edu.au (O.V.); Tel.: +39-0984-493208 (G.C.); +61-2938-51557 (O.V.)

Abstract: Different carbon nanostructures have been explored as functional materials for the development of effective nanomaterials in cancer treatment applications. This review mainly aims to discuss the features, either strength or weakness, of carbon nanohorn (CNH), carbon conical horn-shaped nanostructures of sp² carbon atoms. The interest for these materials arises from their ability to couple the clinically relevant properties of carbon nanomaterials as drug carriers with the negligible toxicity described in vivo. Here, we offer a comprehensive overview of the recent advances in the use of CNH in cancer treatments, underlining the benefits of each functionalization route and approach, as well as the biological performances of either loaded and unloaded materials, while discussing the importance of delivery devices.

Keywords: carbon nanohorns; cancer treatment; drug delivery; functional materials; nanohybrids



Citation: Curcio, M.; Cirillo, G.; Saletta, F.; Michniewicz, F.; Nicoletta, F.P.; Vittorio, O.; Hampel, S.; Iemma, F. Carbon Nanohorns as Effective Nanotherapeutics in Cancer Therapy. *C* **2021**, *7*, 3. <https://dx.doi.org/10.3390/c7010003>

Received: 4 December 2020

Accepted: 23 December 2020

Published: 27 December 2020

Publisher's Note: MDPI stays neutral with regard to jurisdictional claims in published maps and institutional affiliations.



Copyright: © 2020 by the authors. Licensee MDPI, Basel, Switzerland. This article is an open access article distributed under the terms and conditions of the Creative Commons Attribution (CC BY) license (<https://creativecommons.org/licenses/by/4.0/>).

1. Introduction

Nanostructured systems are generally defined as materials with typical size smaller than 100 nm and a high surface area to volume ratio. The characteristic tunable physico-chemical properties make nanoparticles widely employed as vectors of bioactive agents in biomedicine and emerging therapeutic carriers for the treatment of different diseases [1–3]. Nanoparticle systems have been proposed as adjuvant to fight cancer, one of the leading causes of death worldwide [4] which, according to World Health Organization (WHO), is expected to cause 16.5 million deaths with 29.5 million new diagnoses per year in the next two decades [5]. Surgery, chemotherapy and radiotherapy are the three main cancer treatments, but, despite the significant progress made in recent years, an effective strategy for complete tumor cells eradication is still lacking [6–8]. Chemotherapy protocols typically suffer from the unfavorable properties of cytotoxic drugs, such as poor solubility, fast metabolism and clearance, extensive systemic toxicity due to the narrow therapeutic index, and the nonspecific distribution within the body in healthy tissues [9–11]. Similarly, despite the efficacy of radiotherapy protocols, ionizing radiation pose severe risk of toxicity associated with the cumulative radiation dose [12,13]. Alternative therapeutics based on carbon nanomaterials have thus been designed with the aim of addressing these clinical and pharmacological challenges, allowing for the development of more effective clinical protocols [14–16]. Most of the clinically relevant nanostructures are either organic (e.g., polymeric systems, liposome or micelles) or inorganic (e.g., metal and silica nanoparticles,

or nanocrystals) nanoparticles [17–19]. Among them, more than 50 nanodrugs have been approved for different clinical uses including cancer treatment, and more than 70 have entered clinical trials [20,21]. Nevertheless, their effective translation to clinical practice has been hindered by some severe drawbacks, such as their low stability in biological environments or unfavorable pharmacokinetic profiles [22]. Thus, the development of innovative multi-functional materials, combining the key features of different nanostructures, is receiving increasing attention by the research community [23].

Carbon-based nanomaterials (CN) have been widely explored because of their excellent mechanical, thermal, and optical properties, as well as their high biocompatibility after tailored surface functionalization [24–26]. CN were tested for applications in oncology, aiming to address the key challenges of early diagnosis and the efficient treatment of cancers [27–29]. Several research groups have developed highly engineered nanotheranostics by exploiting the ability of the sp^2 carbon surface to interact with multiple copies of drugs via either hydrophobic interactions or π - π stacking [30,31]. Photothermal therapy protocols were proposed taking advantages of the CN absorption pattern in the infrared (IR) or near infrared (NIR) regions, while fluorescence and photoacoustic imaging is possible due to the CN ability to produce fluorescence and transform the energy from a laser into acoustic signals, respectively [32,33]. As a nanocarrier, CN offers advantages to therapy in its ability to accumulate into cancer cells through either passive (enhanced permeability and retention effect—EPR) or active (by surface modification with a specific ligand) targeting [34,35], with the further possibility to confer responsivity to an external stimuli (by introducing appropriate functional groups) for controlling the release of the payload [36,37]. From a chemical point of view, CN are single or multi layered sp^2 carbon lattice differing in size and shape [38,39], which can be classified as nanodots [40], fullerenes (F) [41], nanotubes (CNT) [42], graphene derivatives (G) [43], nanodiamond (ND) [44], and nanohorns (CNH) [45] (Figure 1).

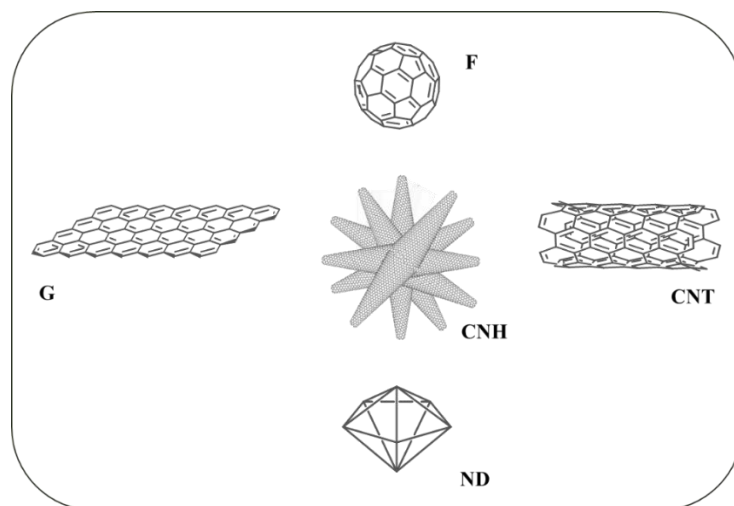


Figure 1. Representation of the main carbon nanostructures.

Nanodiamonds are arrangements of sp^3 carbon atoms in a rigid tetrahedral structure with almost chemical inertness due to the lack of free electrons in the bulk structure [46]. The functionalization of ND via formation of radical species on their surface was exploited as a strategy for the synthesis of biocompatible materials suitable for cancer diagnosis and treatment [47]. Fullerene, consisting of sp^2 carbon atoms arranged in the form of a hollow sphere or ellipsoid, were the first type of CN utilized in biomedicine, where they were and still are employed as theranostics due to their photothermal properties and low toxicity [48]. CNT are sp^2 carbon allotropes with a cylindrical structure and high length-to-diameter ratio. Investigations have determined that while this structure is more conducive to their application as drug carriers in cancer treatment and retains the photothermal properties of fullerene, serious concerns about their long-term toxicity have arisen, leading to debate

regarding their clinical applicability [49–51]. Graphene, single atom sheets of sp^2 carbon atoms arranged in a honeycomb-like structure, is emerging as one of the most promising nanomaterials for application in biological environments because of its ability to couple the typical features of CN with an intrinsic biocompatibility [52–54]. CNH consist of horn shaped nanostructures of sp^2 -bonded carbon atoms, being conceptually imagined as a F subset with CNT chemistry, whose potential applicability in biomedicine was recently explored [55].

In our previous works, we reviewed the advantages of CNT and G derivatives as anticancer nanocarriers in enhancing the efficacy of conventional cytotoxic agents and reversing multi-drug resistance [56,57]. Here, we aim to provide an overview of the recent advances in the use of CNH, a relatively unexplored type of CN which offers interesting solutions for cancer diagnosis and treatment.

2. CNH: A Bridge between Carbon Nanotubes and Fullerenes

From a morphological and topological point of view, CNH consist of a conical front-tip section (cone angle of 120° , main length and diameter of 40–50 and 2–5 nm, respectively) composed of sp^2 carbon atoms arranged in five pentagons (as found in F), with a sixth pentagon forming the CNT-like hexagon walls around the axis [58]. Furthermore, heptagons are present along the axis, to counteract the curvature change of pentagons and confer the typical CNH chemistry [59]. CNH assemble to form aggregates with different morphologies which can be classified in dahlia-like, bud-like or seed-like type [60]. In particular, the dahlia-like CNH, spherical structure with a diameter of 80–100 nm composed of nearly 2000 tubular units, are the most frequently used in nano-oncology applications (Figure 2) [61,62].

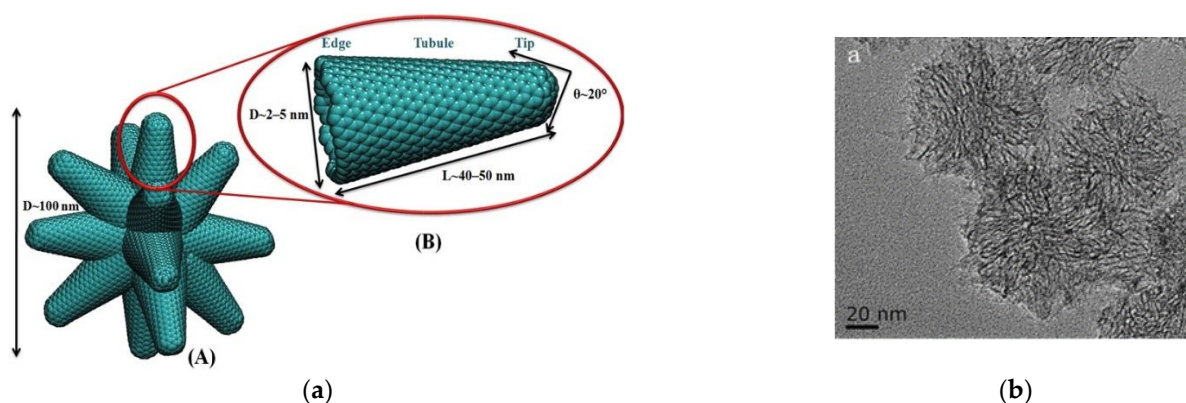


Figure 2. (a) Schematic representation of the morphological features of (A) dahlia like Carbon Nanohorns (CNH) and (B) single CNH, reproduced with permission from [63], Elsevier (2019). (b) Representative TEM image of dahlia like CNH. Reproduced with permission from [64], Elsevier (2015).

The synthesis of CNH is based on the vaporization of a carbon substrate (e.g., graphite) in the absence of any metal catalyst, and the subsequent quenching in an inert atmosphere [65]. Depending on the energy source employed in the vaporization step, three main synthetic methods can be described, namely arc discharge, laser ablation, and joule heating. In all cases, the absence of metal impurities results in a purification step consisting of thermal annealing to remove carbon impurities (in the form of graphite microparticles, fullerenes, giant carbon onions, and amorphous carbon) which results in a remarkably reduced toxicity in biomedical applications [45,66]. This is one of the main advantages of CNH when compared to CNT, alongside the greater specific surface area, higher porosity and higher diameter which allows the free movement of encapsulated molecules and the occurrence of chemical reactions within their inner cavity [67]. Furthermore, the irregular structure of CNH permits the tunable opening of holes at either tips or sidewalls, resulting in a more favorable loading and release of chemotherapeutics [55].

3. Functionalization of CNH for Biomedical Applications

Despite the similarities with other CNs, the chemical features of CNH affect their potential biomedical applications because of their higher reactivity. This is owed to the presence of several defect sites due to loss of aromaticity (e.g., pentagon and heptagon rings) or pyramidal distortion of the sp^2 carbon bonding (e.g., tip and opened tubular end), resulting in easier chemical modification [68].

Covalent and non-covalent functionalization can be determined depending on the type of chemical bond formed during synthesis. The two approaches alter how the π - π network of the CNH surface is preserved or disrupted and therefore the extent to which surface properties such as electrical and thermal conductivity, mechanical strength, and photothermal behavior are retained. The covalent approach guarantees a more stable interaction between CNH and selected functionalizing agents but leads to the formation of sp^3 carbon as perturbing elements of the graphite layer. On the contrary, non-covalent functionalization preserves surface properties but renders a less stable interaction between CNH and derivatizing elements [45] (Figure 3).

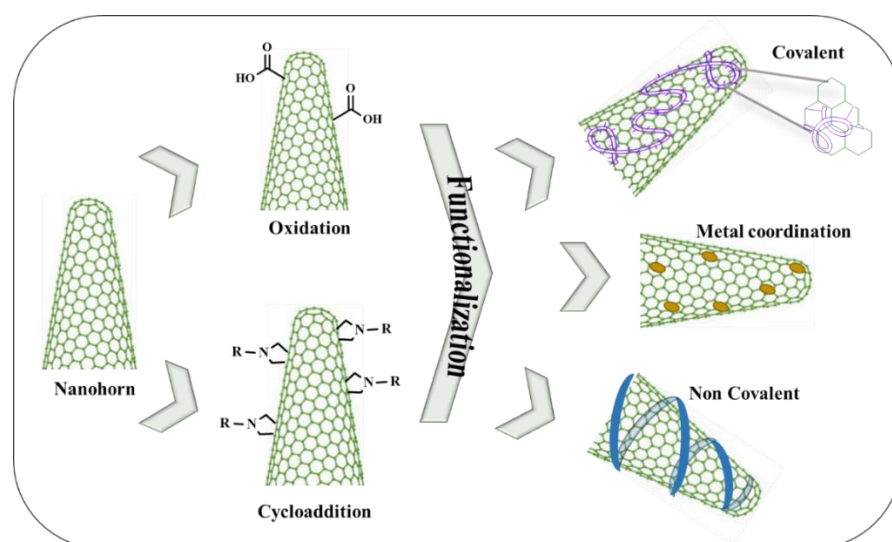


Figure 3. Representation of the main Carbon Nanohorns functionalization routes.

Both approaches can be further classified according to the presence or absence of a preliminary oxidation step, which when carried out causes the formation of holes and oxygen-rich functionalities, such as OH and COOH groups, on the CNH carbon layer. Different strategies can be utilized for CNH oxidation, including treatment with oxidizing acids [69], O_2 at high temperature [70], peroxides [71], or air upon microwave irradiation [72]. The mechanism of oxidation reaction was proposed by Almeida et al. in the case of O_2 treatment [73]. The first step in the oxidation process is the adsorption of oxygen molecules onto CNH defect sites, defined as pentagon rings with higher reactivity. Subsequently, a [2+2] cycloaddition reaction occurs with the formation of peroxide species rapidly undergoing conversion into diketones by breaking of C-C and C-O bonds. Next, further reaction with oxygen molecules lead to the formation of lactones hydrolyzed to carboxyl groups by the nucleophilic attack of H_2O . Different oxidation levels can be obtained by modulating either the concentration of reactant or the reaction time. In detail, the acid treatment results in a low oxygen content while the use of hydrogen peroxide induce carbonyl and carboxyl groups formation by short and long reaction time, respectively, and O_2 treatment prevents the creation of a large number of nanowindows on the CNH surface and thus the loss of structural features [74].

In the next paragraphs, the reviewed studies are divided on the basis of the covalent or non-covalent functionalization, depending on the nature of the chemical bond formed with the functional element responsible for the biological or analytical performance of the

final material. The key parameters considered are the method of synthesis and the in vitro and/or in vivo models employed in their assessment.

3.1. Non-Covalent Functionalization of CNH for Application in Oncology

CNH functionalization through a non-covalent approach involves the π - π stacking interactions with aromatic organic materials [75], the electrostatic interactions [76], the filling of the inner cavity with bioactive molecules [73], as well as the decorating the outer shell with metal nanoparticles such as magnetite [77], titanium [78], palladium [79], and platinum [80] nanoparticles. In most cases, the organic molecule used for CNH derivatization consists of polymeric materials, due to their ability to enhance biocompatibility and confer tailored properties to the carbon nanostructure [81]. Particular types of non-covalent functionalization involve the filling of oxidized CNH with C60 fullerenes [82], or metal nanoparticles such as platinum [83] and gadolinium [84] nanoparticles.

Determining the toxicological and pharmacokinetics profile of the nanostructures is of paramount importance for considering a potential clinical application of CNH. To this regard, the absence of metal impurity was found to be a key determinant to avoid potential carcinogenic risk in cell cultures, as well as in reduced dermal and ocular side-reactions [85], although CNH easily cross the biological barrier and undergo cell internalization via multiple pathways [86,87]. CNH were well tolerated upon either oral ingestion, with a lethal dosage for rats higher than 2000 mg kg⁻¹ of body weight [85] or inhalation [88,89]. Tahara et al. proved negligible toxicity of SWNHs intravenously administered to mice over a 26-week test period [90]. Moreover, while He et al. determined the in vivo fate of CNH which were incorporated within the macrophages by endocytosis and degraded by reactive oxygen species (ROS). Interestingly, this process occurs without determining any inflammatory response due to the low interaction with the key transmembrane protein, the glycoprotein non-metastatic melanoma protein B (GPNMB), which, instead, is involved in the toxicity of different types of nanostructures like CNT [91]. Finally, the wrapping of lipid polyethylene glycol (LPEG) was used to assess the CNH biodistribution [92], obtaining negligible accumulation in the lung, skin, or kidney, while a size-dependent accumulation was observed in liver and spleen.

On the other hand, experimental evidence indicated a direct effect of single walled CNH (SWCNH) on human glioma cell lines, which reduced cell proliferation by blocking the tumor cells in G1 phase and ultimately induced apoptosis [93].

The most relevant and recent examples of non-covalently functionalized CNH proposed for cancer therapy are reported in Table 1. Here, the effectiveness of CNH as biomaterials for cancer treatment was presented by showing either their ability to vectorize drug molecules to the tumor site or the possibility to generate heat upon irradiation thus killing cancer cells. It is evident that most studies focusing on the evaluation of CNH as drug carrier involves the use of cisplatin (CDDP) as chemotherapeutic, while when other drug are employed, authors explored the possibility to combine the delivery efficiency with the NIR absorption properties.

The interest on CDDP vectorization is related to the need of overcoming the acute and cumulative toxic side effects, while preserving the strong anticancer activity of the platinum drug. Several research groups explored the possibility to use carbon nanostructures as base materials for the fabrication of drug delivery vehicles, showing the added values of CNT and CNH [94]. Tubular structures, indeed, offer the possibility to use either the outer surface for loading or the inner surface for filling, with loading efficiency strictly depending on both the CN purification procedure and the solvent [95].

Table 1. Performance of pristine and non-covalent modified CNH for cancer theranostics.

Carrier Features				Biological Features						Ref.
CNH	Derivatizing Agent	Targeting Element	Bioactive Agent (DL%)	Tissue	Cancer Model		Health Model		Performance	
					In Vitro	In Vivo	In Vitro	In Vivo		
CNH	---	---	CDDP ^a (33/50)	---	---	---	---	---	Slow release	[63]
SWCNH	PS	---	---	Brain	U87 U251 U373	---	---	---	Apoptosis	[93]
SWCNH	PF127	---	---	---	---	---	---	---	Photothermal	[96]
SWCNH	PF127	---	---	Breast	MDA-MB-231	---	---	---	Photothermal	[97]
SWCNH	PF127	---	---	Kidney	RENCA	---	---	---	Photothermal	[98]
SWCNH	DCA-HPCS	---	DOX ^b	Breast	4T1	4T1	---	---	Photothermal synergism	[99]
SWCNH	C18PMH/mPEG-PLA	pH	CDDP ^b (66) DOX ^b (44)	Breast Lung	4T1 ---	4T1	---	---	Photothermal synergism	[100]
SWCNH	---	---	ICG ^b (37)	Breast	4T1	4T1	---	---	Photodynamic	[101]
SWCNH	---	---	HYP ^b (52)	Breast	4T1	4T1	---	---	Photodynamic	[102]
SWCNH	---	---	PC ^b (33)	Breast	4T1 MDA-MB-231	4T1	---	Balb/c mice	Photodynamic	[103]
SWCNH	---	---	TSCuPc ^b (36)	Cervix	HeLa	---	---	---	Photodynamic	[104]
oxCNH	DISPE-PEG	P-gp Ab	ETO ^b (40)	Lung	A549 A549R	---	---	---	Photothermal synergism MDR reversal	[105]
¹ oxSWCNH	---	---	---	---	---	---	---	---	Photothermal	[106]
² oxSWCNH	---	---	CDDP ^a (20)	Lung	NCI-H460	---	---	---	Synergism	[61]
oxSWCNH	DISPE-PEG	VEGF mAb	DTX ^b (31)	Breast Liver	MCF7 ---	---	---	H22	Synergism	[107]
oxSWCNH	SA	pH VEGF mAb	DOX ^b (50)	Breast Kidney Liver	MCF7 ---	---	---	HEK293 H22	Synergism	[108]
oxSWCNH	DISPE-PEG	IGF-IR mAb	VCR ^b (38)	Breast Liver	MCF7 ---	---	---	HUVEC H22	Synergism	[64]
² oxSWCNH	PEG-NHBP	---	CDDP ^a (22)	Lung	NCI-H460	---	---	---	Synergism	[109]

¹ Oxidation by HNO₃; ² Oxidation by CO₂ laser; ^a Filling; ^b Wrapping; Ab: Antibody; C18PMH: poly (maleic anhydride-alt-1-octadecene); CDDP: cis-diaminedichloroplatinum(II); CNH: Carbon Nanohorn; DCA: Deoxycholic acid; DISPE: 1,2-Distearoyl-snglycero-3-phosphoethanolamine; DOX: Doxorubicin; DTX: Docetaxel; ETO: Etoposide; HPCS: hydropropyl chitosan; HYP: Hypericin; ICG: Indocyanine green; IGF-IR: insulin-like growth factor-I receptor; mAb: monoclonal Ab; MDR: Multi-drug resistance; mPEG-PLA: methoxypolyethyleneglycol-b-poly-D, L-lactide; ox CNH: Oxidized CNH; oxSWCNH: Oxidized SWCNH; PC: Phycocyanin; PEG: polyethylene glycol; PF: Pluronic F; P-gp: P-glycoprotein; PS: polystyrene; SA: Sodium Alginate; SWCNH: Single-Walled CNH; TSCuPc: Copper(II) phthalocyanine-3,4',4'',4'''-tetrasulfonic acid tetrasodium salt; VEGF: vascular endothelial growth factor; VCR: Vincristine.

The suitability of SWCNH for CDDP encapsulation was proved in a work by Ajima et al. [61], where the slow release (50% in almost 70 h), together with the high CNH uptake by cancer cells, was proposed for the treatment of lung cancer *in vitro*. The same authors proposed a further enhancement to the colloidal stability of oxidized SWCNH (oxSWCNH) in cell culture media by wrapping with a polyethylene glycol (PEG)-peptide aptamer (NHBP-1) conjugate [109]. For a better understanding of the CDDP@CNH efficiency, Almeida et al. [63] conducted experimental and molecular dynamics simulations to predict the stability of the inclusion complex, characterized by the presence of two drug molecules at the tip region. The results indicated that the drug-carrier interaction mainly consisted of van der Waals and electrostatic interactions, the formation of the inclusion complex was thermodynamically favorable, and the opening angle of the cone modulated drug mobility, thus allowing sustained drug release.

As previously mentioned, the effectiveness of CNH in cancer therapy is also related to their NIR absorption ability, allowing the development of both photothermal (PTT) and photodynamic therapy (PDT) protocols. In a photothermal process, the thermal ablation of cancer tissues occurs upon generation of heat by the NIR-irradiated CNH [110], while in a photodynamic protocol cell death is a consequence of the generation of singlet oxygen and other ROS [32]. The ability of CNH to absorb light in the IR region and generate heat [106] was clearly proved to be strongly dependent on the adopted synthetic procedure and the surface modification in experiments assessing the optical properties of sodium alginate (SA) phantoms in the presence of Pluronic F127 (PF127) functionalized CNH [96]. Furthermore, the same authors demonstrated the ability of CNH to act as adjuvant in photothermal therapy with SA phantoms seeded with breast cancer cells [97]. Similar results were obtained *in vitro* in renal cancer cells, where a concentration dependent anticancer efficacy was recorded upon laser irradiation in the presence of PF127 modified SWCNH, with both the laser treatment and exposure to CNH alone being less effective in killing cancer cells [98].

Different studies explored the possibility of combining the photothermal efficacy with carrier features. Specifically, Doxorubicin (DOX) [99,100] and CDDP [100] were loaded via π - π stacking and electrostatic interaction onto the surface of CNH non-covalently functionalized with deoxycholic acid-hydropropyl chitosan conjugate [99] or methoxypolyethyleneglycol-b-poly-D, L-lactide [100], with appropriate photo- and chemo-therapeutic protocols subsequently designed for the treatment of breast [99,100] and lung [100] carcinomas (Figure 4).

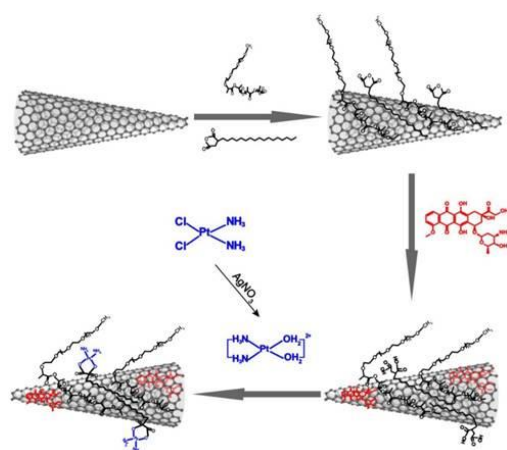


Figure 4. Schematic representation of the preparation of Cisplatin and Doxorubicin dual loaded Single-Walled Carbon Nanohorns. Reproduced from [100]. Ivyspring (2018).

Effective photodynamic therapy protocols were developed by functionalizing the CNH outer surface with photosensitizers, such as indocyanine green (ICG) [101], hypericin (Hyp) [102], phycocyanin (PC) [103], and metal phthalocyanines (MPc) [104]. The resulting

materials, overcoming the limitations of free photosensitizers, such as a tendency to aggregate and to be degraded in physiological environments (ICG, MPc), low water solubility (Hyp), and degradation upon irradiation (PC), were found to be promising tools for the treatment of breast [101–103], and cervical [104] cancer with negligible toxicity in vivo [103] (Figure 5).

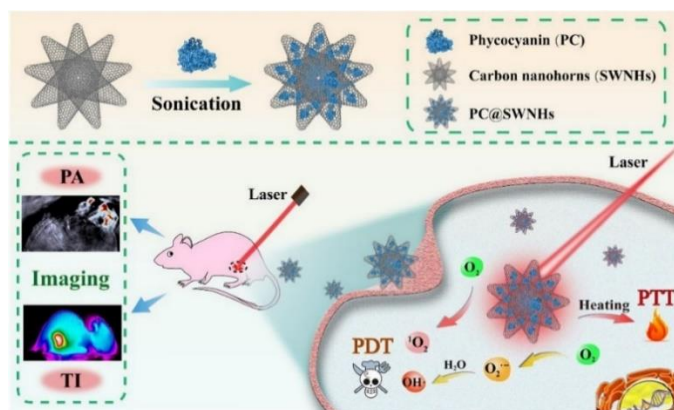


Figure 5. Schematic representation of the route for synthesis of Phycocyanin @ Single Walled Carbon Nanohorns and its use for Near Infrared light-mediated Photothermal / Photodynamic therapy of tumors. Reproduced with permission from [103]. Elsevier (2017).

Active targeting strategies were proposed to improve the selectivity of the nanocarrier, thus enhancing the vectorization efficiency and the anticancer activity.

Humanized anti-vascular endothelial growth factor (anti-VEGF) monoclonal antibody was conjugated to the surface of CNH modified by 1,2-Distearoyl-sn-glycero-3-phosphoethanolamine (DISPE)-PEG or SA, obtaining synergistic effect with the loaded drugs (e.g., Docetaxel—DTX [107] and DOX [108]) in the treatment of breast cancer cells [107,108] in vitro and in in vivo models of liver cancer [108]. In such model, in vitro experiments determined that an acidic pH reminiscent of the tumor environment resulted in a faster and higher DOX release. This led to the hypothesis that drug release could therefore be specific to the tumor site, which was confirmed in vivo by the absence of uptake in healthy kidney cells or of hepatotoxicity, cardiotoxicity, and nephrotoxicity. The same cancer model was used to test DISPE-PEG-CN H modified with an insulin-like growth factor-I receptor (IGF-IR) monoclonal antibody for the vectorization of vincristine (VCR) [64]. Wang et al. [105] proposed the P-gp monoclonal antibody as a targeting ligand for the treatment of lung cancer, addressing multi-drug resistance (MDR) insurgence. In fact, upon exposure to etoposide (ETO), overexpression of membrane efflux pumps was induced, resulting in drug intracellular concentration and thus the cytotoxic efficiency, being dramatically reduced. The proposed therapeutic strategy strongly inhibited the activity of the membrane transporters, and the anticancer efficacy was restored.

3.2. Covalent Functionalization of CNH for Application in Oncology

The covalent functionalization of outer surface is proposed to improve the performance of CNH as delivery vehicle because the stable interaction with the derivatization moieties allows the properties of the final device to be finely tuned according to the specific therapeutic needs. The most relevant and recent examples of covalently functionalized CNH proposed for cancer therapy are reported in Table 2.

The explored strategies to chemically modify CNH mainly consist in condensation reaction on oxCNH or cycloaddition reaction on the surface of pristine CNH.

Table 2. Performance of covalent modified CNH for cancer theranostics.

CNH	Carrier Features				Biological Features					Ref.	
	Derivatization		Targeting	Bioactive Agent (DL%)	Cancer Model		Health Model		Performance		
	Derivatizing Agent	Synthesis			Tissue	In Vitro	In Vivo	In Vitro			In Vivo
¹ oxSWCNH	AET CdSe/ZnS QDs	Condensation (EDC)/ Coordination	---	---	Breast	MDA-MB-231	---	---	---	High uptake	[111]
					Brain	U-87					
					Bladder	AY-27					
¹ oxSWCNH	CDDP	Condensation (EDC)	---	---	Bladder	AY-27	---	---	---	High uptake Photothermal	[112]
	---	---	---	CDDP ^a							
	AET CdSe/ZnS QDs	Condensation (EDC)/ Coordination	---	---							
¹ oxSWCNH	AET CdSe/ZnS QDs	Condensation (EDC)/ Coordination	---	CDDP ^a (19)	Bladder	AY-27	---	---	---	Synergism Fluorescence Imaging	[113]
² oxCNH	PEI	Condensation (EDC)	Magnetic	MAG	Cervix	HeLa	---	---	---	Photothermal	[114]
² oxCNH	PEI	Condensation (EDC)	Magnetic FA	MAG	Epidermis	KB	---	FHs173We	---	Photothermal	[55]
² oxCNH	Liposome-AVI-BIOT- PEI	Condensation (EDC)	Magnetic	MAG	Cervix	HeLa	---	GP8 SV40	Mice	Photothermal	[115]
³ oxSWCNH	BSA/ZnPc	Condensation (EDC)/Wrapping	—	—	Modified Fibroblast	5RP7	5RP7	---	---	Photothermal	[116]
CNH	PSMA mAb	Cycloaddition	PSMA mAb	CDDP ^b (1.3)	Prostate	PC-3	---	---	---	Synergism	[117]
CNH	PAMAM	Cycloaddition	---	siRNA ^b DTX ^c	Prostate	LNCaP	---	---	---	Synergism	[118]
CNH	PAMAM/ AuNPs	Cycloaddition/Coordination	---	siRNA ^b	Prostate	PC3	---	---	---	Synergism	[119]

¹ Oxidation by HNO₃; ² Oxidation by O₂ flow; ³ Oxidation by H₂O₂; ^a Filling; ^b Wrapping; ^c Mixing; AET: cysteamine hydrochloride; AuNPs: Gold Nanoparticles; AV: Avidin; BIOT: Biotin; BSA: Bovine Serum Albumin; CDDP: cis-diaminedichloroplatinum(II); CNH: Carbon Nanohorn; DTX: Docetaxel; EDC: N-(3-dimethylaminopropyl)-N-ethylcarbodiimidehydrochloride; FA: Folic Acid; mAb: Monoclonal Antibody; MAG: magnetic iron nanoparticles; oxCNH: Oxidized CNH; PAMAM: polyamidoamine dendrimer; PEI: Polyethylenimine; PMSA: prostate-specific membrane antigen; QDs: Quantum Dots; SWCNH: Single-Walled CNH; ZnPc: Zinc phthalocyanine.

In the first case, the COOH and OH groups formed in the oxidation step undergo further chemical derivatizations, such as nucleophilic/electrophilic amidation, esterification, and thiolation reactions through acyl chloride or carbodiimide chemistry [72].

Zimmermann et al. [111] used the covalent functionalization with cysteamine hydrochloride (AET) as a ligand for CdSe/ZnS Quantum Dots (QD) to investigate the intracellular fate of oxCNH in glioblastoma, breast cancer, and bladder transitional carcinoma *in vitro*. Through flow cytometry they demonstrated that CNH were internalized by endocytosis with a cell type-dependent uptake rate. Furthermore, while at the first experimental timepoint (60 min) the main observed cellular localization was cytosolic, a significant amount of nanoparticle was evident in the nuclei after 24 h. More interestingly, the internalization was still observed after 24 h, corresponding to the time required for SWCNH aggregation in the cell culture media.

Another approach involves the use of bioactive species as derivatizing agents. A CDDP nanocarrier obtained by covalent conjugation of the cytotoxic drug onto the surface of oxCNH, observing a significant reduction in the efficiency of combined photo- and chemo-therapy [112]. To further investigate this issue, the efficiency of the CDDP-CN H conjugate was compared with a carrier prepared by inserting the drug in the inner cavity of the carbon nanostructure, and used the functionalization with CdSe/ZnS QDs to study the cellular uptake pathways (Figure 6) [113].

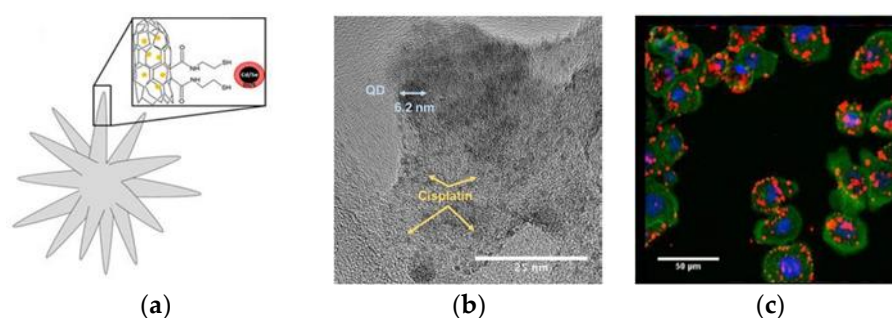


Figure 6. (a) Representation of Cisplatin-Carbon Nanohorns/Quantum Dots (CDDP-CN H/CdSe/ZnS QDs); (b) TEM images of CDDP-CN H/CdSe/ZnS QDs; (c) Internalization of CDDP-CN H/CdSe/ZnS QDs in AY-27 cells. Reproduced with permission from [113]. Elsevier (2018).

The covalent functionalization did not significantly affect the internalization rate, but the anticancer efficacy was demonstrated to depend by the different kinetics of drug release. Upon covalent conjugation negligible amount of drug was released, resulting in a lower efficiency compared to the free drug. The faster release of the CDDP inclusion complex was found to be more cytotoxic upon NIR irradiation, allowing better control of drug distribution between cancerous and healthy tissues compared to the administration of free CDDP. By combining improved cytotoxicity and fluorescence, nanocarriers with these design features were proposed as nanotheranostic vehicles in the treatment of bladder cancer [113].

Another interesting functionalization method derives from the covalent “grafting to” and “grafting from” of polymeric materials onto the CNH surface [56]. The “grafting to” the surface is performed by natural or synthetic polymers linked to chemical functionalities available of CNH outer shell [120], while the second approach involves the binding of suitable initiator systems on CNH and the *in situ* formation of synthetic polymeric materials by anionic, cationic, radical, or atom transfer radical polymerization [121].

Polyethylenimine (PEI) was used for the covalent functionalization of nanocomplexes composed of oxCNH obtained by treatment with oxygen flow and magnetite nanoparticles (MAG) [114]. The obtained system took advantages from the water affinity of PEI and the ability of MAG to enhance cellular uptake upon exposure to an external magnetic field, and was successfully tested in a cervical cancer model. The same authors proposed further upgrades to the nanovehicles through the use of folic acid as a targeting unit for

the treatment of human epidermal carcinoma [55], or PEI functionalized liposomes for the development of supramolecular nanotransporters [115]. In the latter case, by using fluorescent probe, the authors obtained a temporal and spatial control on the payload delivery both in vitro and in vivo.

As discussed in regards to non-covalent functionalization routes, covalent modifications of CNH were also developed for photodynamic (PDT) and photothermal (PTT) cancer therapy. [116]. The PTT features of CNH were combined with the PDT properties of zinc phthalocyanine covalently attached to the surface of oxCNH, obtained by treatment with oxygen peroxide. Effective cancer ablation in vitro and in vivo was obtained through a final coating of the structure with bovine serum albumin.

Covalent derivatization methods of pristine CNH include the formation of fluorinated CNH by treatment with F_2 at high temperature [122], and amino-CNH by refluxing in NH_3 in the presence of $NaNH_2$ [123], respectively. In this case, the obtained CNH derivative can undergo further modification reactions by nucleophilic substitution or amidation reactions, respectively. Carbamate chemistry [124], the addition of aryl diazonium salts [125] 1,3-dipolar cycloaddition [126], and copper-catalyzed alkyne-azide cycloaddition [127] reactions were also employed as derivatization procedures of pristine CNH.

Cycloaddition reactions were explored for the covalent conjugation of targeting unit, namely the anti-PSMA D2B Ab, for the vectorization of CDDP to prostate cancer cells [117]. These reactions were also employed to fabricate polyamidoamine dendrimer (PAMAM) based delivery system for siRNA, due to the ability of PAMAMs to both enhance CNH water affinity preventing any unfavorable aggregation process, and interact with RNA molecules via electrostatic binding [118,119].

The typical 1,3-cycloaddition involves the reaction between CNH and the suitable aldehyde and amino acid in an appropriate organic solvent [128]. Aldehyde and amino acid reacted in situ to form an azomethine ylides undergoing coupling with CNH and preserving, at the same time, the integrity of the sp^2 surface lattice [129]. This method, extensively exploited by Prato and co-workers to obtain different CNT and G derivatives for biomedical applications, can be useful for orthogonal substitutions, either in the presence of in the absence of simultaneous oxidation procedures [130,131].

Finally, it should be mentioned that, in the efforts to find innovative solvent-free and “green” chemistry approaches for covalent CNH functionalization, microwave-assisted reactions are emerging as cost-effective methods for the preparation of CNH derivative with high yields and purity [72].

4. Conclusions and Perspectives

Improving cytotoxic drugs' efficacy in cancer treatment by tailored nanomaterials is attracting great attention in different research fields, from chemistry and materials science to biology and medicine. Among others, the favorable properties of CN used to the develop nanocarriers based on F, CNT, and GO have shown improved efficiency against cancer cells with significant reduction of toxicity to healthy tissues. Here, we highlight the performances of a specific class of CN, namely CNH, which, due to their physicochemical and biological features, can be conceptually considered as a bridge between F, CNT and GO, coupling the advantages of CNT (high cell uptake) with those of F and GO (reduced toxicity). These materials are still not widely utilized in biomedicine, although the encouraging results published over the last few years, as summarized in Table 3, are opening interesting opportunities for the development of effective nanocarriers.

The studies reviewed in this paper can be organized according to the two main classes of CNH (pristine vs. oxidized), and the type of functionalization approach (covalent vs. non-covalent). The outcomes of each study are expressed as success (%) in cancer treatment by two categories, namely the drug synergisms and the suitability for phototherapy treatments, although different performances can be described including the improvement of the release profile, the interference with the apoptotic pathways, and the induction of MDR reversal.

Table 3. Main outcome of the studies covered in this review.

CNH	Approach	Ref.	Total Studies *	Derivatizing Agent	Reaction	Targeting	Drug	Cancer Model	Efficacy	Side-Toxicity	Performance
										% Studies #	% Success #
CNH	Non covalent	[63] [93] [96] [97] [98] [99] [100] [101] [102] [103] [104]	12	None (42) PF (25) Other (33)	None (33) Wrapping (77)	None (83) Stimuli (17)	None (35) CDDP (25) DOX (8) ICG (8) HYP (8) PC (8) TsCuPc (8)	None (18) Breast (50) Brain (8) Kidney (8) Lung (8) Cervix (8)	Vitro (75) Vivo (50)	0	Release (8) Apoptosis (8) Synergism (25) Phototherapy (75)
	Covalent	[117] [118] [119]	3	PAMAM (67) Ab (33)	Cycloaddition (100)	Ab (33)	CDDP (33) SiRNA (66) DTX (33)	Prostate (100)	Vitro (100)		Synergism (100)
oxCNH	Non covalent	[61] [64] [105, 106] [107] [108] [109]	9	None (22) dPEG (67) SA (11)	None (22) Wrapping (78)	None (33) Ab (66) pH (11)	None (11) CDDP (22) DTX (22) DOX (11) VCR (22) ETO (11)	None (11) Lung (33) Breast (33) Liver (22)	Vitro (67) Vivo (33)	22	Synergism (78) Phototherapy (22) MDR reversal (11)
oxCNH	Covalent	[55] [111] [112] [113] [114] [115] [116]	11	None (9) QDs (45) PEI (27) BSA (9) CDDP (9)	Condensation (100)	Magnetic (27) FA (9)	None (85) CDDP (27) MAG (27)	Bladder (45) Cervix (18) Breast (9) Brain (9) Epidermis (9) Fibroblast (9)	Vitro (100) Vivo (9)	18	Synergism (36) Phootherapy (63)

* A single ref may cover multiple studies simultaneously. # calculated over the total studies. Ab: Antibody; BSA: Bovine Serum Albumin; CDDP: cis-diaminedichloroplatinum(II); DOX: Doxorubicin; dPEG: Polyethylene glycol derivatives; DTX: Docetaxel; ETO: Etoposide; FA: Folic acid; HYP: Hypericin; ICG: Indocyanine green; MAG: magnetic iron nanoparticles; PAMAM: polyamidoamine; PC: phycocyanin; PEI: Polyethylenimine; PF: Pluronic F; QDs: Quantum Dots; SA: Sodium Alginate; TSCuPc: Copper(II) phthalocyanine-3,4',4''-tetrasulfonic acid tetrasodium salt; VCR: Vincristine.

Finally, to give a comprehensive overview of the study heterogeneity and for a better discussion of the results, the carrier's features, as well as the loaded drug and the tested cancer model, are reported as amount (%) of studies, with a single research article covering multiple studies simultaneously. Most studies involving pristine CNH report on non-covalent functionalization approaches, while covalent functionalization routes are more relevant in the case of oxCNH, due to the ability of such functionalities to undergo derivatization via condensation reaction with tailored chemical species of either low or high molecular weight.

Interestingly, pristine CNH are often used alone in the absence of loaded drug, due to their ability to promote photothermal ablation of cancer cells even in the absence of any derivatizing agent, while nanocarriers for the delivery of CDDP and DOX in the presence of siRNA were obtained by cycloaddition on the same nanostructures. oxCNH suitably modified by either covalent or non-covalent methods was mainly proposed as cargo to synergize CDDP efficiency with reduced side-toxicity, although covalent functionalization routes (mainly with PEG derivatives) were proposed for the enhancement of anticancer performance by phototherapy protocols without the loading of any cytotoxic drug.

Finally, a relevant number of studies proposed the possibility to confer a targeting effect by exploiting the different pH environment of healthy vs. cancer tissues, applying an external magnetic field as driving force for the vectorization, or using Ab moieties to selectively target cancer cells.

However, it should be highlighted that despite the very promising results obtained in in vitro models of diseases, the lack of adequate studies using suitable in vivo models strongly restricts current understanding of how these structures behave in biological systems. This is the main issue to be addressed before hypothesizing a translation into pre-clinical or clinical trials. This restriction does not diminish however, the currently available findings which are broadly positive. In particular, the hypothesized low side-toxicity of CNH based devices indicate that these studies should be used as a starting point for experimental protocols aiming to couple multidisciplinary and complementary expertise for the development of innovative functional nanomaterials for fighting cancer.

Funding: This research received no external funding.

Institutional Review Board Statement: Not applicable.

Informed Consent Statement: Not applicable.

Data Availability Statement: Not applicable.

Conflicts of Interest: The authors declare no conflict of interest.

References

1. De Jong, W.H.; Borm, P.J.A. Drug delivery and nanoparticles: Applications and hazards. *Int. J. Nanomed.* **2008**, *3*, 133–149. [[CrossRef](#)] [[PubMed](#)]
2. Kim, B.Y.S.; Rutka, J.T.; Chan, W.C.W. Current concepts: Nanomedicine. *N. Engl. J. Med.* **2010**, *363*, 2434–2443. [[CrossRef](#)] [[PubMed](#)]
3. Stylianopoulos, T.; Jain, R.K. Design considerations for nanotherapeutics in oncology. *Nanomed. Nanotechnol. Biol. Med.* **2015**, *11*, 1893–1907. [[CrossRef](#)] [[PubMed](#)]
4. Bray, F.; Ferlay, J.; Soerjomataram, I.; Siegel, R.L.; Torre, L.A.; Jemal, A. Global Cancer Statistics 2018: GLOBOCAN Estimates of Incidence and Mortality Worldwide for 36 Cancers in 185 Countries. *Ca Cancer J. Clin.* **2018**, *68*, 394–424. [[CrossRef](#)]
5. International Agency for Research on Cancer. *Cancer Tomorrow*; International Agency for Research on Cancer: Lyon, France, 2019.
6. Norouzi, M.; Amerian, M.; Atyabi, F. Clinical applications of nanomedicine in cancer therapy. *Drug Discov. Today* **2020**, *25*, 107–125. [[CrossRef](#)]
7. Lytton-Jean, A.K.R.; Kauffman, K.J.; Kaczmarek, J.C.; Langer, R. Cancer nanotherapeutics in clinical trials. In *Cancer Treatment and Research*; Springer: Cham, Switzerland, 2015; Volume 166, pp. 293–322.
8. Pradeep, P.; Kumar, P.; Choonara, Y.E.; Pillay, V. Targeted nanotechnologies for cancer intervention: A patent review (2010–2016). *Expert Opin. Ther. Pat.* **2017**, *27*, 1005–1019. [[CrossRef](#)]
9. Da Silva, C.G.; Peters, G.J.; Ossendorp, F.; Cruz, L.J. The potential of multi-compound nanoparticles to bypass drug resistance in cancer. *Cancer Chemother. Pharmacol.* **2017**, *80*, 881–894. [[CrossRef](#)]

10. Guo, X.; Zhuang, Q.; Ji, T.; Zhang, Y.; Li, C.; Wang, Y.; Li, H.; Jia, H.; Liu, Y.; Du, L. Multi-functionalized chitosan nanoparticles for enhanced chemotherapy in lung cancer. *Carbohydr. Polym.* **2018**, *195*, 311–320. [[CrossRef](#)]
11. Weeks, J.C.; Catalano, P.J.; Cronin, A.; Finkelman, M.D.; Mack, J.W.; Keating, N.L.; Schrag, D. Patients' expectations about effects of chemotherapy for advanced cancer. *N. Engl. J. Med.* **2012**, *367*, 1616–1625. [[CrossRef](#)]
12. Peitzsch, C.; Cojoc, M.; Hein, L.; Kurth, I.; Mäbert, K.; Trautmann, F.; Klink, B.; Schröck, E.; Wirth, M.P.; Krause, M.; et al. An Epigenetic Reprogramming Strategy to Resensitize Radioresistant Prostate Cancer Cells. *Cancer Res.* **2016**, *76*, 2637–2651. [[CrossRef](#)]
13. Huang, Y.; Fan, C.Q.; Dong, H.; Wang, S.M.; Yang, X.C.; Yang, S.M. Current applications and future prospects of nanomaterials in tumor therapy. *Int. J. Nanomed.* **2017**, *12*, 1815–1825. [[CrossRef](#)] [[PubMed](#)]
14. Alsaab, H.O.; Alghamdi, M.S.; Alotaibi, A.S.; Alzhrani, R.; Alwuthaynani, F.; Althobaiti, Y.S.; Almalki, A.H.; Sau, S.; Iyer, A.K. Progress in clinical trials of photodynamic therapy for solid tumors and the role of nanomedicine. *Cancers* **2020**, *12*, 2793. [[CrossRef](#)] [[PubMed](#)]
15. Liang, R.; Chen, Y.; Huo, M.; Zhang, J.; Li, Y. Sequential catalytic nanomedicine augments synergistic chemodrug and chemodynamic cancer therapy. *Nanoscale Horiz.* **2019**, *4*, 890–901. [[CrossRef](#)]
16. Bhise, K.; Sau, S.; Alsaab, H.; Kashaw, S.K.; Tekade, R.K.; Iyer, A.K. Nanomedicine for cancer diagnosis and therapy: Advancement, success and structure-activity relationship. *Ther. Deliv.* **2017**, *8*, 1003–1018. [[CrossRef](#)]
17. Faraji, A.H.; Wipf, P. Nanoparticles in cellular drug delivery. *Bioorgan. Med. Chem.* **2009**, *17*, 2950–2962. [[CrossRef](#)]
18. Parveen, S.; Misra, R.; Sahoo, S.K. Nanoparticles: A boon to drug delivery, therapeutics, diagnostics and imaging. *Nanomed. Nanotechnol. Biol. Med.* **2012**, *8*, 147–166. [[CrossRef](#)]
19. Lee, D.E.; Koo, H.; Sun, I.C.; Ryu, J.H.; Kim, K.; Kwon, I.C. Multifunctional nanoparticles for multimodal imaging and theragnosis. *Chem. Soc. Rev.* **2012**, *41*, 2656–2672. [[CrossRef](#)]
20. Ventola, C.L. Progress in nanomedicine: Approved and investigational nanodrugs. *Pharm. Ther.* **2017**, *42*, 742–755.
21. Bobo, D.; Robinson, K.J.; Islam, J.; Thurecht, K.J.; Corrie, S.R. Nanoparticle-Based Medicines: A Review of FDA-Approved Materials and Clinical Trials to Date. *Pharm. Res.* **2016**, *33*, 2373–2387. [[CrossRef](#)]
22. Rodriguez-Lorenzo, L.; Rafiee, S.D.; Reis, C.; Milosevic, A.; Moore, T.L.; Balog, S.; Rothen-Rutishauser, B.; Ruegg, C.; Petri-Fink, A. A rational and iterative process for targeted nanoparticle design and validation. *Colloids Surf. B Biointerfaces* **2018**, *171*, 579–589. [[CrossRef](#)]
23. Wegst, U.G.K.; Bai, H.; Saiz, E.; Tomsia, A.P.; Ritchie, R.O. Bioinspired structural materials. *Nat. Mater.* **2015**, *14*, 23–36. [[CrossRef](#)] [[PubMed](#)]
24. Shibu, E.S.; Hamada, M.; Murase, N.; Biju, V. Nanomaterials formulations for photothermal and photodynamic therapy of cancer. *J. Photochem. Photobiol. C Photochem. Rev.* **2013**, *15*, 53–72. [[CrossRef](#)]
25. Yamashita, T.; Yamashita, K.; Nabeshi, H.; Yoshikawa, T.; Yoshioka, Y.; Tsunoda, S.I.; Tsutsumi, Y. Carbon nanomaterials: Efficacy and safety for nanomedicine. *Materials* **2012**, *5*, 350–363. [[CrossRef](#)] [[PubMed](#)]
26. Maharaj, D.; Bhushan, B. Friction, wear and mechanical behavior of nano-objects on the nanoscale. *Mater. Sci. Eng. R Rep.* **2015**, *95*, 1–43. [[CrossRef](#)]
27. Bianco, A.; Kostarelos, K.; Prato, M. Opportunities and challenges of carbon-based nanomaterials for cancer therapy. *Expert Opin. Drug Deliv.* **2008**, *5*, 331–342. [[CrossRef](#)]
28. Loh, K.P.; Ho, D.; Chiu, G.N.C.; Leong, D.T.; Pastorin, G.; Chow, E.K.H. Clinical Applications of Carbon Nanomaterials in Diagnostics and Therapy. *Adv. Mater.* **2018**, *30*, 1802368. [[CrossRef](#)]
29. Yang, C.; Denno, M.E.; Pyakurel, P.; Venton, B.J. Recent trends in carbon nanomaterial-based electrochemical sensors for biomolecules: A review. *Anal. Chim. Acta* **2015**, *887*, 17–37. [[CrossRef](#)]
30. Teradal, N.L.; Jelinek, R. Carbon Nanomaterials in Biological Studies and Biomedicine. *Adv. Healthc. Mater.* **2017**, *6*, 1700574. [[CrossRef](#)]
31. Mehra, N.K.; Jain, A.K.; Nahar, M. Carbon nanomaterials in oncology: An expanding horizon. *Drug Discov. Today* **2018**, *23*, 1016–1025. [[CrossRef](#)]
32. MacDonald, I.J.; Dougherty, T.J. Basic principles of photodynamic therapy. *J. Porphyr. Phthalocyanines* **2001**, *5*, 105–129. [[CrossRef](#)]
33. Sawdon, A.; Weydemeyer, E.; Peng, C.A. Tumor photothermolysis: Using carbon nanomaterials for cancer therapy. *Eur. J. Nanomed.* **2013**, *5*, 131–140. [[CrossRef](#)]
34. Augustine, S.; Singh, J.; Srivastava, M.; Sharma, M.; Das, A.; Malhotra, B.D. Recent advances in carbon based nanosystems for cancer theranostics. *Biomater. Sci.* **2017**, *5*, 901–952. [[CrossRef](#)] [[PubMed](#)]
35. Biagiotti, G.; Fedeli, S.; Tuci, G.; Luconi, L.; Giambastiani, G.; Brandi, A.; Pisaneschi, F.; Cicchi, S.; Paoli, P. Combined therapies with nanostructured carbon materials: There is room still available at the bottom. *J. Mater. Chem. B* **2018**, *6*, 2022–2035. [[CrossRef](#)] [[PubMed](#)]
36. Spizzirri, U.G.; Curcio, M.; Cirillo, G.; Spataro, T.; Vittorio, O.; Picci, N.; Hampel, S.; Iemma, F.; Nicoletta, F.P. Recent advances in the synthesis and biomedical applications of nanocomposite hydrogels. *Pharmaceutics* **2015**, *7*, 413–437. [[CrossRef](#)] [[PubMed](#)]
37. Liu, Z.; Robinson, J.T.; Tabakman, S.M.; Yang, K.; Dai, H.J. Carbon materials for drug delivery & cancer therapy. *Mater. Today* **2011**, *14*, 316–323. [[CrossRef](#)]
38. Nasir, S.; Hussein, M.Z.; Zainal, Z.; Yusof, N.A. Carbon-based nanomaterials/allotropes: A glimpse of their synthesis, properties and some applications. *Materials* **2018**, *11*, 295. [[CrossRef](#)]

39. Vedhanarayanan, B.; Praveen, V.K.; Das, G.; Ajayaghosh, A. Hybrid materials of 1D and 2D carbon allotropes and synthetic π -systems. *NPG Asia Mater.* **2018**, *10*, 107–126. [[CrossRef](#)]
40. Wu, Y.F.; Wu, H.C.; Kuan, C.H.; Lin, C.J.; Wang, L.W.; Chang, C.W.; Wang, T.W. Multi-functionalized carbon dots as theranostic nanoagent for gene delivery in lung cancer therapy. *Sci. Rep.* **2016**, *6*, 21170. [[CrossRef](#)]
41. Lin, H.S.; Matsuo, Y. Functionalization of [60] fullerene through fullerene cation intermediates. *Chem. Commun.* **2018**, *54*, 11244–11259. [[CrossRef](#)]
42. Tasis, D.; Tagmatarchis, N.; Bianco, A.; Prato, M. Chemistry of carbon nanotubes. *Chem. Rev.* **2006**, *106*, 1105–1136. [[CrossRef](#)]
43. Rao, C.N.R.; Sood, A.K.; Subrahmanyam, K.S.; Govindaraj, A. Graphene: The new two-dimensional nanomaterial. *Angew. Chem. Int. Ed.* **2009**, *48*, 7752–7777. [[CrossRef](#)] [[PubMed](#)]
44. Mochalin, V.N.; Shenderova, O.; Ho, D.; Gogotsi, Y. The properties and applications of nanodiamonds. *Nat. Nanotechnol.* **2012**, *7*, 11–23. [[CrossRef](#)] [[PubMed](#)]
45. Karousis, N.; Suarez-Martinez, I.; Ewels, C.P.; Tagmatarchis, N. Structure, Properties, Functionalization, and Applications of Carbon Nanohorns. *Chem. Rev.* **2016**, *116*, 4850–4883. [[CrossRef](#)] [[PubMed](#)]
46. Kaur, R.; Badea, I. Nanodiamonds as novel nanomaterials for biomedical applications: Drug delivery and imaging systems. *Int. J. Nanomed.* **2013**, *8*, 203–220. [[CrossRef](#)]
47. Liu, K.K.; Cheng, C.L.; Chang, C.C.; Chao, J.I. Biocompatible and detectable carboxylated nanodiamond on human cell. *Nanotechnology* **2007**, *18*, 325102. [[CrossRef](#)]
48. Bakry, R.; Vallant, R.M.; Najam-Ul-Haq, M.; Rainer, M.; Szabo, Z.; Huck, C.W.; Bonn, G.K. Medicinal applications of fullerenes. *Int. J. Nanomed.* **2007**, *2*, 639–649.
49. De Volder, M.F.L.; Tawfick, S.H.; Baughman, R.H.; Hart, A.J. Carbon nanotubes: Present and future commercial applications. *Science* **2013**, *339*, 535–539. [[CrossRef](#)]
50. Bianco, A.; Kostarelos, K.; Partidos, C.D.; Prato, M. Biomedical applications of functionalised carbon nanotubes. *Chem. Commun.* **2005**, *5*, 571–577. [[CrossRef](#)]
51. Fabbro, C.; Ali-Boucetta, H.; Ros, T.D.; Kostarelos, K.; Bianco, A.; Prato, M. Targeting carbon nanotubes against cancer. *Chem. Commun.* **2012**, *48*, 3911–3926. [[CrossRef](#)]
52. Byun, J. Emerging frontiers of graphene in biomedicine. *J. Microbiol. Biotechnol.* **2015**, *25*, 145–151. [[CrossRef](#)]
53. Feng, L.; Liu, Z. Graphene in biomedicine: Opportunities and challenges. *Nanomedicine* **2011**, *6*, 317–324. [[CrossRef](#)] [[PubMed](#)]
54. Chung, C.; Kim, Y.K.; Shin, D.; Ryoo, S.R.; Hong, B.H.; Min, D.H. Biomedical applications of graphene and graphene oxide. *Acc. Chem. Res.* **2013**, *46*, 2211–2224. [[CrossRef](#)] [[PubMed](#)]
55. Chechetka, S.A.; Zhang, M.; Yudasaka, M.; Miyako, E. Physicochemically functionalized carbon nanohorns for multi-dimensional cancer elimination. *Carbon* **2016**, *97*, 45–53. [[CrossRef](#)]
56. Cirillo, G.; Peitzsch, C.; Vittorio, O.; Curcio, M.; Farfalla, A.; Voli, F.; Dubrovskaya, A.; Iemma, F.; Kavallaris, M.; Hampel, S. When polymers meet carbon nanostructures: Expanding horizons in cancer therapy. *Future Med. Chem.* **2019**, *11*, 2205–2231. [[CrossRef](#)] [[PubMed](#)]
57. Curcio, M.; Farfalla, A.; Saletta, F.; Valli, E.; Pantuso, E.; Nicoletta, F.P.; Iemma, F.; Vittorio, O.; Cirillo, G. Functionalized carbon nanostructures versus drug resistance: Promising scenarios in cancer treatment. *Molecules* **2020**, *25*, 2102. [[CrossRef](#)] [[PubMed](#)]
58. Azami, T.; Kasuya, D.; Yuge, R.; Yudasaka, M.; Iijima, S.; Yoshitake, T.; Kubo, Y. Large-scale production of single-wall carbon nanohorns with high purity. *J. Phys. Chem. C* **2008**, *112*, 1330–1334. [[CrossRef](#)]
59. Zhu, S.; Xu, G. Single-walled carbon nanohorns and their applications. *Nanoscale* **2010**, *2*, 2538–2549. [[CrossRef](#)]
60. Chen, D.; Dougherty, C.A.; Zhu, K.; Hong, H. Theranostic applications of carbon nanomaterials in cancer: Focus on imaging and cargo delivery. *J. Control. Release* **2015**, *210*, 230–245. [[CrossRef](#)]
61. Ajima, K.; Yudasaka, M.; Murakami, T.; Maigné, A.; Shiba, K.; Iijima, S. Carbon nanohorns as anticancer drug carriers. *Mol. Pharm.* **2005**, *2*, 475–480. [[CrossRef](#)]
62. Guerra, J.; Herrero, M.A.; Vázquez, E. Carbon nanohorns as alternative gene delivery vectors. *RSC Adv.* **2014**, *4*, 27315–27321. [[CrossRef](#)]
63. Almeida, E.R.; De Souza, L.A.; De Almeida, W.B.; Dos Santos, H.F. Molecular dynamics of carbon nanohorns and their complexes with cisplatin in aqueous solution. *J. Mol. Graph. Model.* **2019**, *89*, 167–177. [[CrossRef](#)] [[PubMed](#)]
64. Li, N.; Zhao, Q.; Shu, C.; Ma, X.; Li, R.; Shen, H.; Zhong, W. Targeted killing of cancer cells in vivo and in vitro with IGF-IR antibody-directed carbon nanohorns based drug delivery. *Int. J. Pharm.* **2015**, *478*, 644–654. [[CrossRef](#)] [[PubMed](#)]
65. Aryee, E.; Dalai, A.K.; Adjaye, J. Maximization of carbon nanohorns production via the Arc discharge method for hydrotreating application. *J. Nanosci. Nanotechnol.* **2017**, *17*, 4784–4791. [[CrossRef](#)]
66. Albert, K.; Hsu, H.Y. Carbon-based materials for photo-triggered theranostic applications. *Molecules* **2016**, *21*, 1585. [[CrossRef](#)]
67. Kagkoura, A.; Tagmatarchis, N. Carbon nanohorn-based electrocatalysts for energy conversion. *Nanomaterials* **2020**, *10*, 1407. [[CrossRef](#)]
68. Zhang, M.; Yudasaka, M.; Ajima, K.; Miyawaki, J.; Iijima, S. Light-assisted oxidation of single-wall carbon nanohorns for abundant creation of oxygenated groups that enable Chemical modifications with proteins to enhance biocompatibility. *ACS Nano* **2007**, *1*, 265–272. [[CrossRef](#)]
69. Aryee, E.; Dalai, A.K.; Adjaye, J. Functionalization and characterization of carbon nanohorns (CNHs) for hydrotreating of gas oils. *Top. Catal.* **2014**, *57*, 796–805. [[CrossRef](#)]

70. Pagona, G.; Tagmatarchis, N.; Fan, J.; Yudasaka, M.; Iijima, S. Cone-end functionalization of carbon nanohorns. *Chem. Mater.* **2006**, *18*, 3918–3920. [[CrossRef](#)]
71. Sahu, S.R.; Rikka, V.R.; Jagannatham, M.; Haridoss, P.; Chatterjee, A.; Gopalan, R.; Prakash, R. Synthesis of graphene sheets from single walled carbon nanohorns: Novel conversion from cone to sheet morphology. *Mater. Res. Express* **2017**, *4*, 035008. [[CrossRef](#)]
72. Yoshida, S.; Sano, M. Microwave-assisted chemical modification of carbon nanohorns: Oxidation and Pt deposition. *Chem. Phys. Lett.* **2006**, *433*, 97–100. [[CrossRef](#)]
73. Almeida, E.R.; De Souza, L.A.; De Almeida, W.B.; Dos Santos, H.F. Chemically Modified Carbon Nanohorns as Nanovectors of the Cisplatin Drug: A Molecular Dynamics Study. *J. Chem. Inf. Model.* **2020**, *60*, 500–512. [[CrossRef](#)] [[PubMed](#)]
74. Agresti, F.; Barison, S.; Famengo, A.; Pagura, C.; Fedele, L.; Rossi, S.; Bobbo, S.; Rancan, M.; Fabrizio, M. Surface oxidation of single wall carbon nanohorns for the production of surfactant free water-based colloids. *J. Colloid Interface Sci.* **2018**, *514*, 528–533. [[CrossRef](#)] [[PubMed](#)]
75. Muñoz, J.; Sansores, E.; Olea, A.; Valenzuela, E. The role of aromaticity on the building of nanohybrid materials functionalized with metalated (Au(III), Ag(III), Cu(III)) extended porphyrins and single-walled carbon nanohorns: A theoretical study. *Int. J. Quantum Chem.* **2013**, *113*, 1034–1046. [[CrossRef](#)]
76. Aoyagi, M.; Yudasaka, M.; Minamikawa, H.; Asakawa, M.; Masuda, M.; Shimizu, T.; Iijima, S. Quantitative analyses of PEGylated phospholipids adsorbed on single walled carbon nanohorns by high resolution magic angle spinning 1H NMR. *Carbon* **2016**, *101*, 213–217. [[CrossRef](#)]
77. Utsumi, S.; Urita, K.; Kanoh, H.; Yudasaka, M.; Suenaga, K.; Iijima, S.; Kaneko, K. Preparing a magnetically responsive single-wall carbon nanohorn colloid by anchoring magnetite nanoparticles. *J. Phys. Chem. B* **2006**, *110*, 7165–7170. [[CrossRef](#)] [[PubMed](#)]
78. Tu, W.; Lei, J.; Ding, L.; Ju, H. Sandwich nanohybrid of single-walled carbon nanohorns-TiO₂-porphyrin for electrocatalysis and amperometric biosensing towards chloramphenicol. *Chem. Commun.* **2009**, *28*, 4227–4229. [[CrossRef](#)]
79. Itoh, T.; Danjo, H.; Sasaki, W.; Urita, K.; Bekyarova, E.; Arai, M.; Imamoto, T.; Yudasaka, M.; Iijima, S.; Kanoh, H.; et al. Catalytic activities of Pd-tailored single wall carbon nanohorns. *Carbon* **2008**, *46*, 172–175. [[CrossRef](#)]
80. Liu, Y.; Brown, C.M.; Neumann, D.A.; Geohegan, D.B.; Puzos, A.A.; Rouleau, C.M.; Hu, H.; Styers-Barnett, D.; Krasnov, P.O.; Yakobson, B.I. Metal-assisted hydrogen storage on Pt-decorated single-walled carbon nanohorns. *Carbon* **2012**, *50*, 4953–4964. [[CrossRef](#)]
81. Mountrichas, G.; Pispas, S.; Ichihashi, T.; Yudasaka, M.; Iijima, S.; Tagmatarchis, N. Polymer covalent functionalization of carbon nanohorns using bulk free radical polymerization. *Chem. A Eur. J.* **2010**, *16*, 5927–5933. [[CrossRef](#)]
82. Ajima, K.; Yudasaka, M.; Suenaga, K.; Kasuya, D.; Azami, T.; Iijima, S. Material Storage Mechanism in Porous Nanocarbon. *Adv. Mater.* **2004**, *16*, 397–401. [[CrossRef](#)]
83. Yuge, R.; Ichihashi, T.; Shimakawa, Y.; Kubo, Y.; Yudasaka, M.; Iijima, S. Preferential deposition of Pt nanoparticles inside single-walled carbon nanohorns. *Adv. Mater.* **2004**, *16*, 1420–1423. [[CrossRef](#)]
84. Miyawaki, J.; Matsumura, S.; Yuge, R.; Murakami, T.; Sato, S.; Tomida, A.; Tsuruo, T.; Ichihashi, T.; Fujinami, T.; Irie, H.; et al. Biodistribution and ultrastructural localization of single-walled carbon nanohorns determined in vivo with embedded Gd₂O₃ labels. *ACS Nano* **2009**, *3*, 1399–1406. [[CrossRef](#)] [[PubMed](#)]
85. Miyawaki, J.; Yudasaka, M.; Azami, T.; Kubo, Y.; Iijima, S. Toxicity of single-walled carbon nanohorns. *ACS Nano* **2008**, *2*, 213–226. [[CrossRef](#)] [[PubMed](#)]
86. Moreno-Lanceta, A.; Medrano-Bosch, M.; Melgar-Lesmes, P. Single-walled carbon nanohorns as promising nanotube-derived delivery systems to treat cancer. *Pharmaceutics* **2020**, *12*, 850. [[CrossRef](#)]
87. Hifni, B.; Khan, M.; Devereux, S.J.; Byrne, M.H.; Quinn, S.J.; Simpson, J.C. Investigation of the Cellular Destination of Fluorescently Labeled Carbon Nanohorns in Cultured Cells. *ACS Appl. Bio Mater.* **2020**, *3*, 6790–6801. [[CrossRef](#)]
88. Schramm, F.; Lange, M.; Hoppmann, P.; Heutelbeck, A. Cytotoxicity of carbon nanohorns in different human cells of the respiratory system. *J. Toxicol. Environ. Health Part. A* **2016**, *79*, 1085–1093. [[CrossRef](#)]
89. Lynch, R.M.; Voy, B.H.; Glass, D.F.; Mahurin, S.M.; Zhao, B.; Hu, H.; Saxton, A.M.; Donnell, R.L.; Cheng, M.D. Assessing the pulmonary toxicity of single-walled carbon nanohorns. *Nanotoxicology* **2007**, *1*, 157–166. [[CrossRef](#)]
90. Tahara, Y.; Miyawaki, J.; Zhang, M.; Yang, M.; Waga, I.; Iijima, S.; Irie, H.; Yudasaka, M. Histological assessments for toxicity and functionalization-dependent biodistribution of carbon nanohorns. *Nanotechnology* **2011**, *22*, 265106. [[CrossRef](#)]
91. He, B.; Shi, Y.; Liang, Y.; Yang, A.; Fan, Z.; Yuan, L.; Zou, X.; Chang, X.; Zhang, H.; Wang, X.; et al. Single-walled carbon-nanohorns improve biocompatibility over nanotubes by triggering less protein-initiated pyroptosis and apoptosis in macrophages. *Nat. Commun.* **2018**, *9*, 1–21. [[CrossRef](#)]
92. Zhang, M.; Yamaguchi, T.; Iijima, S.; Yudasaka, M. Size-dependent biodistribution of carbon nanohorns in vivo. *Nanomed. Nanotechnol. Biol. Med.* **2013**, *9*, 657–664. [[CrossRef](#)]
93. Li, Y.; Zhang, J.; Zhao, M.; Shi, Z.; Chen, X.; He, X.; Han, N.; Xu, R. Single-wall carbon nanohorns (SWNHs) inhibited proliferation of human glioma cells and promoted its apoptosis. *J. Nanoparticle Res.* **2013**, *15*, 1861. [[CrossRef](#)]
94. Nowacki, M.; Wisniewski, M.; Werengowska-Cieciewicz, K.; Roszek, K.; Czarnecka, J.; Lakomska, I.; Kloskowski, T.; Tyloch, D.; Debski, R.; Pietkun, K.; et al. Nanovehicles as a novel target strategy for hyperthermic intraperitoneal chemotherapy: A multidisciplinary study of peritoneal carcinomatosis. *Oncotarget* **2015**, *6*, 22776–22798. [[CrossRef](#)] [[PubMed](#)]
95. Werengowska-Cieciewicz, K.; Wiśniewski, M.; Terzyk, A.P.; Gurtowska, N.; Olkowska, J.; Kloskowski, T.; Drewa, T.A.; Kielkowska, U.; Druzyński, S. Nanotube-mediated efficiency of cisplatin anticancer therapy. *Carbon* **2014**, *70*, 46–58. [[CrossRef](#)]

96. Sarkar, S.; Gurjarpadhye, A.A.; Rylander, C.G.; Rylander, M.N. Optical properties of breast tumor phantoms containing carbon nanotubes and nanohorns. *J. Biomed. Opt.* **2011**, *16*, 051304. [[CrossRef](#)] [[PubMed](#)]
97. Whitney, J.; Dewitt, M.; Whited, B.M.; Carswell, W.; Simon, A.; Rylander, C.G.; Rylander, M.N. 3D viability imaging of tumor phantoms treated with single-walled carbon nanohorns and photothermal therapy. *Nanotechnology* **2013**, *24*, 275102. [[CrossRef](#)]
98. Whitney, J.R.; Sarkar, S.; Zhang, J.; Do, T.; Young, T.; Manson, M.K.; Campbell, T.A.; Poretzky, A.A.; Rouleau, C.M.; More, K.L.; et al. Single walled carbon nanohorns as photothermal cancer agents. *Lasers Surg. Med.* **2011**, *43*, 43–51. [[CrossRef](#)]
99. Chen, D.; Wang, C.; Jiang, F.; Liu, Z.; Shu, C.; Wan, L.J. In vitro and in vivo photothermally enhanced chemotherapy by single-walled carbon nanohorns as a drug delivery system. *J. Mater. Chem. B* **2014**, *2*, 4726–4732. [[CrossRef](#)]
100. Yang, J.; Su, H.; Sun, W.; Cai, J.; Liu, S.; Chai, Y.; Zhang, C. Dual chemodrug-loaded single-walled carbon nanohorns for multimodal imaging-guided chemo-photothermal therapy of tumors and lung metastases. *Theranostics* **2018**, *8*, 1966–1984. [[CrossRef](#)]
101. Gao, C.; Dong, P.; Lin, Z.; Guo, X.; Jiang, B.P.; Ji, S.; Liang, H.; Shen, X.C. Near-Infrared Light Responsive Imaging-Guided Photothermal and Photodynamic Synergistic Therapy Nanoplatform Based on Carbon Nanohorns for Efficient Cancer Treatment. *Chem. A Eur. J.* **2018**, *24*, 12827–12837. [[CrossRef](#)]
102. Gao, C.; Jian, J.; Lin, Z.; Yu, Y.X.; Jiang, B.P.; Chen, H.; Shen, X.C. Hypericin-Loaded Carbon Nanohorn Hybrid for Combined Photodynamic and Photothermal Therapy in Vivo. *Langmuir* **2019**, *35*, 8228–8237. [[CrossRef](#)]
103. Lin, Z.; Jiang, B.P.; Liang, J.; Wen, C.; Shen, X.C. Phycocyanin functionalized single-walled carbon nanohorns hybrid for near-infrared light-mediated cancer phototheranostics. *Carbon* **2019**, *143*, 814–827. [[CrossRef](#)]
104. Jiang, B.P.; Hu, L.F.; Shen, X.C.; Ji, S.C.; Shi, Z.; Liu, C.J.; Zhang, L.; Liang, H. One-step preparation of a water-soluble carbon nanohorn/phthalocyanine hybrid for dual-modality photothermal and photodynamic therapy. *ACS Appl. Mater. Interfaces* **2014**, *6*, 18008–18017. [[CrossRef](#)] [[PubMed](#)]
105. Wang, J.; Wang, R.; Zhang, F.; Yin, Y.; Mei, L.; Song, F.; Tao, M.; Yue, W.; Zhong, W. Overcoming multidrug resistance by a combination of chemotherapy and photothermal therapy mediated by carbon nanohorns. *J. Mater. Chem. B* **2016**, *4*, 6043–6051. [[CrossRef](#)] [[PubMed](#)]
106. Gurova, O.A.; Omelyanchuk, L.V.; Dubatolova, T.D.; Antokhin, E.I.; Eliseev, V.S.; Yushina, I.V.; Okotrub, A.V. Synthesis and modification of carbon nanohorns structure for hyperthermic application. *J. Struct. Chem.* **2017**, *58*, 1205–1212. [[CrossRef](#)]
107. Zhao, Q.; Li, N.; Shu, C.; Li, R.; Ma, X.; Li, X.; Wang, R.; Zhong, W. Docetaxel-loaded single-wall carbon nanohorns using anti-VEGF antibody as a targeting agent: Characterization, in vitro and in vivo antitumor activity. *J. Nanoparticle Res.* **2015**, *17*, 207. [[CrossRef](#)]
108. Ma, X.; Shu, C.; Guo, J.; Pang, L.; Su, L.; Fu, D.; Zhong, W. Targeted cancer therapy based on single-wall carbon nanohorns with doxorubicin in vitro and in vivo. *J. Nanoparticle Res.* **2014**, *16*, 2497. [[CrossRef](#)]
109. Matsumura, S.; Ajima, K.; Yudasaka, M.; Iijima, S.; Shiba, K. Dispersion of cisplatin-loaded carbon nanohorns with a conjugate comprised of an artificial peptide aptamer and polyethylene glycol. *Mol. Pharm.* **2007**, *4*, 723–729. [[CrossRef](#)]
110. Shanmugam, V.; Selvakumar, S.; Yeh, C.S. Near-infrared light-responsive nanomaterials in cancer therapeutics. *Chem. Soc. Rev.* **2014**, *43*, 6254–6287. [[CrossRef](#)]
111. Zimmermann, K.A.; Inglefield, D.L., Jr.; Zhang, J.; Dorn, H.C.; Long, T.E.; Rylander, C.G.; Rylander, M.N. Single-walled carbon nanohorns decorated with semiconductor quantum dots to evaluate intracellular transport. *J. Nanoparticle Res.* **2014**, *16*, 2078. [[CrossRef](#)]
112. DeWitt, M.R.; Pekkanen, A.M.; Robertson, J.; Rylander, C.G.; Rylander, M.N. Influence of hyperthermia on efficacy and uptake of carbon nanohorn-cisplatin conjugates. *J. Biomech. Eng.* **2014**, *136*, 021003. [[CrossRef](#)]
113. Isaac, K.M.; Sabaraya, I.V.; Ghousifam, N.; Das, D.; Pekkanen, A.M.; Romanovicz, D.K.; Long, T.E.; Saleh, N.B.; Rylander, M.N. Functionalization of single-walled carbon nanohorns for simultaneous fluorescence imaging and cisplatin delivery in vitro. *Carbon* **2018**, *138*, 309–318. [[CrossRef](#)]
114. Chechetka, S.A.; Pichon, B.; Zhang, M.; Yudasaka, M.; Bégin-Colin, S.; Bianco, A.; Miyako, E. Multifunctional carbon nanohorn complexes for cancer treatment. *Chem. Asian J.* **2015**, *10*, 160–165. [[CrossRef](#)] [[PubMed](#)]
115. Chechetka, S.A.; Yuba, E.; Kono, K.; Yudasaka, M.; Bianco, A.; Miyako, E. Magnetically and near-infrared light-powered supramolecular nanotransporters for the remote control of enzymatic reactions. *Angew. Chem. Int. Ed.* **2016**, *55*, 6476–6481. [[CrossRef](#)] [[PubMed](#)]
116. Zhang, M.; Murakami, T.; Ajima, K.; Tsuchida, K.; Sandanayaka, A.S.D.; Ito, O.; Iijima, S.; Yudasaka, M. Fabrication of ZnPc/protein nanohorns for double photodynamic and hyperthermic cancer phototherapy. *Proc. Natl. Acad. Sci. USA* **2008**, *105*, 14773–14778. [[CrossRef](#)]
117. Lucío, M.I.; Opri, R.; Pinto, M.; Scarsi, A.; Fierro, J.L.G.; Meneghetti, M.; Fracasso, G.; Prato, M.; Vázquez, E.; Herrero, M.A. Targeted killing of prostate cancer cells using antibody-drug conjugated carbon nanohorns. *J. Mater. Chem. B* **2017**, *5*, 8821–8832. [[CrossRef](#)]
118. Pérez-Martínez, F.C.; Carrión, B.; Lucío, M.I.; Rubio, N.; Herrero, M.A.; Vázquez, E.; Ceña, V. Enhanced docetaxel-mediated cytotoxicity in human prostate cancer cells through knockdown of cofilin-1 by carbon nanohorn delivered siRNA. *Biomaterials* **2012**, *33*, 8152–8159. [[CrossRef](#)]

119. Guerra, J.; Herrero, M.A.; Carrión, B.; Pérez-Martínez, F.C.; Lucío, M.; Rubio, N.; Meneghetti, M.; Prato, M.; Ceña, V.; Vázquez, E. Carbon nanohorns functionalized with polyamidoamine dendrimers as efficient biocarrier materials for gene therapy. *Carbon* **2012**, *50*, 2832–2844. [[CrossRef](#)]
120. Cirillo, G.; Caruso, T.; Hampel, S.; Haase, D.; Puoci, F.; Ritschel, M.; Leonhardt, A.; Curcio, M.; Iemma, F.; Khavrus, V.; et al. Novel carbon nanotube composites by grafting reaction with water-compatible redox initiator system. *Colloid Polym. Sci.* **2013**, *291*, 699–708. [[CrossRef](#)]
121. Zhu, S.; Li, J.; Chen, Y.; Chen, Z.; Chen, C.; Li, Y.; Cui, Z.; Zhang, D. Grafting of graphene oxide with stimuli-responsive polymers by using ATRP for drug release. *J. Nanoparticle Res.* **2012**, *14*, 1132. [[CrossRef](#)]
122. Hattori, Y.; Kanoh, H.; Okino, F.; Touhara, H.; Kasuya, D.; Yudasaka, M.; Iijima, S.; Kaneko, K. Direct thermal fluorination of single wall carbon nanohorns. *J. Phys. Chem. B* **2004**, *108*, 9614–9618. [[CrossRef](#)]
123. Isobe, H.; Tanaka, T.; Maeda, R.; Noiri, E.; Solin, N.; Yudasaka, M.; Iijima, S.; Nakamura, E. Preparation, purification, characterization, and cytotoxicity assessment of water-soluble, transition-metal-free carbon nanotube aggregates. *Angew. Chem. Int. Ed.* **2006**, *45*, 6676–6680. [[CrossRef](#)] [[PubMed](#)]
124. Lacotte, S.; García, A.; Décossas, M.; Al-Jamal, W.T.; Li, S.; Kostarelos, K.; Muller, S.; Prato, M.; Dumortier, H.; Bianco, A. Interfacing functionalized carbon nanohorns with primary phagocytic cells. *Adv. Mater.* **2008**, *20*, 2421–2426. [[CrossRef](#)]
125. Pagona, G.; Karousis, N.; Tagmatarchis, N. Aryl diazonium functionalization of carbon nanohorns. *Carbon* **2008**, *46*, 604–610. [[CrossRef](#)]
126. Tagmatarchis, N.; Maigné, A.; Yudasaka, M.; Iijima, S. Functionalization of carbon nanohorns with azomethine ylides: Towards solubility enhancement and electron-transfer processes. *Small* **2006**, *2*, 490–494. [[CrossRef](#)] [[PubMed](#)]
127. Vizueté, M.; Gómez-Escalonilla, M.J.; Fierro, J.L.G.; Yudasaka, M.; Iijima, S.; Vartanian, M.; Iehl, J.; Nierengarten, J.F.; Langa, F. A soluble hybrid material combining carbon nanohorns and C₆₀. *Chem. Commun.* **2011**, *47*, 12771–12773. [[CrossRef](#)] [[PubMed](#)]
128. Cioffi, C.; Campidelli, S.; Brunetti, F.G.; Meneghetti, M.; Prato, M. Functionalisation of carbon nanohorns. *Chem. Commun.* **2006**, *20*, 2129–2131. [[CrossRef](#)]
129. Herrero, M.A.; Prato, M. Recent advances in the covalent functionalization of carbon nanotubes. *Mol. Cryst. Liq. Cryst.* **2008**, *483*, 21–32. [[CrossRef](#)]
130. Quintana, M.; Spyrou, K.; Grzelczak, M.; Browne, W.R.; Rudolf, P.; Prato, M. Functionalization of Graphene via 1,3-Dipolar Cycloaddition. *ACS Nano* **2010**, *4*, 3527–3533. [[CrossRef](#)]
131. Battigelli, A.; Menard-Moyon, C.; Da Ros, T.; Prato, M.; Bianco, A. Endowing carbon nanotubes with biological and biomedical properties by chemical modifications. *Adv. Drug Deliv. Rev.* **2013**, *65*, 1899–1920. [[CrossRef](#)]